Chapter Number xxx

Multiresolutional Filter Application for Spatial Information Fusion in Robot Navigation

Özer Ciftcioglu
Delft University of Technology
The Netherlands

1. Introduction

Robot navigation is one of the major fields of study in autonomous robotics (Oriolio, G., Ulivi, G. et al., 1998; Beetz, M., Arbuckle, T. et al., 2001; Wang, M. & Liu, J.N.K., 2004). In the present work, application of a multiresolutional filter for spatial information fusion in vision robot navigation is described. The novelty of the research is the enhanced estimation of the spatial sensory information in autonomous robotics by means of wavelet decomposition into multiresolutional levels and the fusion of the processed information while the processing takes place at the respective levels. Although wavelet-based information fusion is used in different applications (Hong, L., 1994; Hsin, H.C. & Li, A.C., 2006), its application in robotics is not common in literature. A wavelet-based filtering application in perceptual robotics is articulated earlier where human perception was central to the research. In the present work, optimal vision signal estimation for an autonomous robot is presented, where vision information is obtained by appropriate shaping of the visual sensory information and optimal estimation is obtained by a multiresolutional filter. One of the peculiarities of the research is essentially the wavelet-based dynamic filtering rather than static wavelet decomposition for image analysis or off-line decomposition for signal analysis. A multiresolutional dynamic filtering is a rather complex system. In this system vector form of wavelet decomposition is required as briefly mentioned by Hong (Hong, L., 1993) where the description of a multi-sensor fusion rather than wavelet decomposition was central to the study. In contrast to (Hong, L., 1993), in this work the multiresolutional dynamic filtering is central to the study together with the emphasis on application peculiarities in autonomous robotics; namely, several options for vector-wise operations are pointed out and one of the options is described in detail. Also, in autonomous robotics, the estimation of angular velocity is not a measurable quantity and it has to be estimated from the measurable state variables so that obstacle avoidance problem is taken care of. Therefore, the angular velocity estimation in real-time is a critical task in autonomous robotics and from this viewpoint the multiresolutional spatial information fusion process is desirable for enhanced robot performance. For the fusion process extended Kalman filtering can be used and is actually used in the present study. Perceptual vision employed in this study is one of the vision alternatives in robotics providing several essential possibilities characterizing the robot as to its performance. Especially perceptual robotics is gaining importance in the last decade as to

its expected connection to human-like behaviour. The organization of the work is as follows. After brief description of wavelet transform, a detailed description of vector wavelet decomposition and inverse wavelet transform is presented with a vector decomposition and reconstruction example. The optimal processing of decomposed information is briefly given as proposed by Hong (Hong, L., 1993). This is followed by fusion of information from different multiresolutional levels that it is based on minimum fusion error covariance. Finally, autonomous robot implementation is described with the experimental results illustrating the sensory information and estimated trajectory thereby demonstrating the effective navigation of a moving robot. The work is accomplished in a virtual environment with the intention of realization in real-life environment in due course as the work constitutes a common place for diverse robotics areas like autonomous, perceptual, vision, cognitive etc.

2. Perceptual vision and multiresolutional decomposition

In this work a robot with perceptual vision is considered. The robot is provided with vision via sensors which can measure the distance between the robot and the forward direction via rays interacting with the environment. The rays can be conveniently shaped within a vision cone with a narrow solid cone angle. This is illustrated in figure 1.

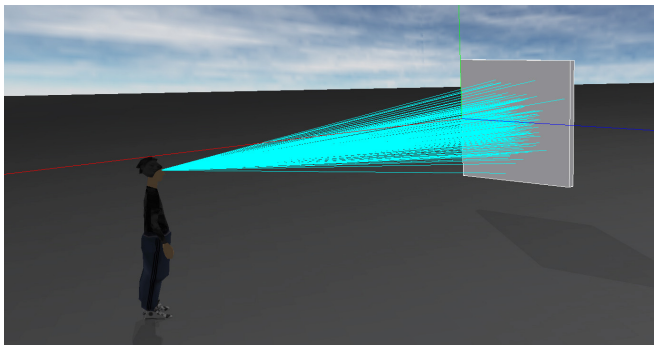

Fig. 1 Perception measurement in the virtual reality. Perception is determined as probability by means of the rays impinging on an object.

Vision rays interact with the environment which includes side walls and hindrance along the forward direction. For an environment a permanent fictive vertical planes at certain threshold distances are considered. If a distance is more than the threshold value it is taken to be the threshold value. This means if the real environment is in front of that fictive plane the actual distance measured by the sensor is considered as distance. If the measured distances are beyond the predetermined threshold distances the robot moves forward without any angular velocity. The position estimation of robot is accomplished by means of Kalman filtering via the states of the robot navigation dynamics as presented earlier (Ciftcioglu, Ö., Bittermann, M.S. et al., 2007). In this work, the enhanced estimation of the states is investigated via wavelet transform (Mallat, S.G., 1989; Ogden, T., 1997; Mallat, S., 1999; Percival, D.B. & Walden, A.T., 2000).

2.1 Wavelets

The novel feature of wavelets is that they are localized in time and frequency as to signals. This behaviour makes them convenient for the analysis of non-stationary signals. It is an elementary introduction of wavelets by introducing a scaling function, such that

$$\phi(t) = \sqrt{2}\sum_k h_k \phi(2t-k) \tag{1}$$

A counterpart of this function is called mother wavelet function obtained from

$$\psi(t) = \sqrt{2}\sum_k g_k \phi(2t-k) \tag{2}$$

where l_k and h_k are related via the equation

$$g_k = (-1)^k h_{1-k} \tag{3}$$

In signal processing literature (3) is known as the *quadrature mirror relation* and the filter $\boldsymbol{h}$ and $\boldsymbol{g}$ as *quadrature mirror filters*. The coefficients g_k and h_k that is, the quadrature mirror filters are used to compute the wavelet transform. $\phi(t)$ and $\psi(t)$ form orthogonal functional low-pass and high-pass filters respectively which are spaces in $L_2(\mathfrak{R})$ where inner product of functions with finite energy is defined. The orthogonal spaces satisfy the property

$$\phi_{m,k}(t) \cup \psi(t)_{m,k} = \phi_{m+1,k}(t) \tag{4}$$

where

$$\phi_{m,k}(t) = 2^{m/2}\phi(2^m t - k) \tag{5}$$

$$\psi_{m,k}(t) = 2^{m/2}\psi(2^m t - k) \tag{6}$$

m=0 constitutes the coarsest scale. The simplest filter coefficients are known as Haar filter and given by

$$\begin{aligned} h_h &= [h_1 \;\; h_2] = \frac{1}{\sqrt{2}}[1 \quad 1] \\ g_h &= [g_1 \;\; g_2] = \frac{1}{\sqrt{2}}[1 \quad -1] \end{aligned} \tag{7}$$

Haar wavelets have generally practical value for several reasons. The building blocks in decomposition are discontinuous functions that are not effective approximating smooth functions. However, because of their very simple form, especially in real-time measurement applications their value is eminent. The present application constitutes such an application and demonstrates their effectiveness. More about wavelets can be found in the literature (Mallat, S.G., 1989; Ogden, T., 1997; Mallat, S., 1999; Vidakovic, B., 1999; Percival, D.B. & Walden, A.T., 2000).

2.2 The Kalman filter

Kalman filter is an estimator of states of a dynamic system with a minimal error variance and in this sense it is optimal. The dynamic system is given in a form which is terminologically referred to as state-space:

$$x(k+1) = A(k)x(k) + B(k)w(k) \tag{8}$$

$$z(k) = C(k)x(k) + v(k) \tag{9}$$

where A is the system matrix, B process noise matrix, C is the measurement matrix. Further, w*(k)* and v*(k)* are Gaussian process noise and measurement noise respectively with the properties

$$E\{w(k)\} = 0$$
$$E\{w(k)\,w(l)^T\} = Q(k)\ for\ \ k = l \tag{10}$$
$$= 0\ otherwise$$

$$E\{v(k)\} = 0$$
$$E\{v(k)\,v(l)^T\} = R(k)\ for\ \ k = l \tag{11}$$
$$= 0\ otherwise$$

In this work, Kalman filter is used to combine the information from the measurements at different resolutional levels and enhance the state estimation rather than to employ single measurement at each time-step. The estimation by Kalman filter is accomplished recursively. As to the conventional notations used in the literature (Anderson, B.D.O. & Moore, J.B., 1979; Maybeck, P.S., 1979; Brown, R.G. & Hwang, Y.C., 1997; Zarchan, P. & Musoff, H., 2005; Shalom, Y.B., Li, X.R. et al., 2006; Simon, D., 2006), the recursion is carried out by standard matrix equations given below.

$$x(k+1\,|\,k) = A(k)x(k\,|\,k) \tag{12}$$

$$P(k+1\,|\,k) = A(k)P(k\,|\,k)A(k)^T + B(k)Q(k)B(k)^T \tag{13}$$

$$K(k+1) = \frac{P(k+1\,|\,k)C(k+1)^T}{C(k+1)P(k+1\,|\,k)C(k+1)^T + R(k+1)} \tag{14}$$

So that the updated state variables and covariance matrix are

$$x(k+1\,|\,k+1) = x(k+1\,|\,k) + \tag{15}$$
$$([z(k+1) - C(k+1)x(k+1\,|\,k)]K(k+1)$$

$$P(k+1\,|\,k+1) = [I - K(k+1)C(k+1)]P(k+1\,|\,k) \tag{16}$$

2.3 The Multiresolutional filter

N-level multiresolutional dynamic system can be described by

$$\begin{aligned} &x^{[N]}(k_N+1) = A^{[N]}(k_N)x^{[N]}(k_N), \\ &z^{[i]}(k_i) = C^{[i]}(k_i)x^{[i]}(k_i) + v^{[i]}(k_i) \\ &i = 1,\ldots,N \end{aligned} \tag{17}$$

where i=N is the highest resolution level, so that

$$\begin{aligned} &E\left[w^{[N]}(k_N)\right] = 0, \\ &E\left[w^{[N]}(k_N)w^{[N]}(l_N)^T\right] = Q^{[N]}(k_N), \quad k = l \\ &\qquad\qquad\qquad\qquad = 0 \quad k \neq l \end{aligned} \tag{18}$$

Referring to the measurements $z^{(\text{Shalom, Y.B., Li, X.R. et al.})}(k_i)$ at different resolution levels, we write

$$\begin{aligned} &E\left[w^{[i]}(k_i)\right] = 0, \\ &E\left[w^{[i]}(k_i)w^{[i]}(l_i)^T\right] = Q^{[i]}(k_i), \quad k = l \\ &\qquad\qquad\qquad\qquad = 0 \quad k \neq l \end{aligned} \tag{19}$$

and

$$\begin{aligned} &E\left[v^{[i]}(k_i)\right] = 0, \\ &E\left[v^{[i]}(k_i)v^{[i]}(l_i)^T\right] = R^{[i]}(k_i), \quad k = l \\ &\qquad\qquad\qquad\qquad = 0 \quad k \neq l \end{aligned} \tag{20}$$

Measurements at different resolution levels can be carried out in different ways. One way of doing this is shown with the following scheme.

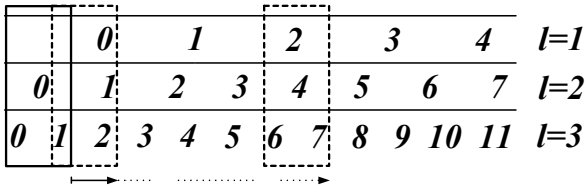

where different resolution levels are indicated by *l*=1,2,3 while the highest resolution level is for l=3. In this implementation a moving window is used. When samples 0 and 1 are available in the window at *l*=3, sample 0 is calculated at the resolution level *l*=1 by wavelet decomposition; when the samples 1 and 2 are available at *l*=3, the sample 1 is calculated at the resolution level *l*=2 which is followed by the calculated sample 0 at the level *l*=1 using the samples 0 and 1 at the level *l*=2. In this way the moving window multiresolutional dynamic filtering can be executed.

Another alternative for the multiresolutional measurements can be accomplished by the following scheme.

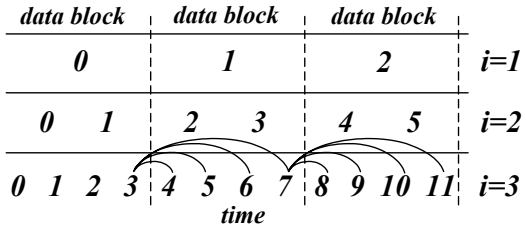

In this scheme each data block at the highest resolution level (i=3) contains 4 samples and at this very level, the Kalman filtering estimations within the data block are carried out using the last data sample of the preceding block, together with the respective data samples within the block. Namely, for instance using the data sample 3 at the level i=3, 1-step ahead, 2-step ahead, 3-step ahead and 4-step ahead Kalman predictions are made and as the data samples 4, 5,6, and 7 are available, the respective estimations are made in sequence at the time points where the measurements are available; that is at the time points 4, 5, 6, and 7.

Another scheme of measurements at different resolution levels are shown in figure 2 and the wavelet decomposition of state variables in a data block is shown in figure 3. This is the actual scheme implemented in this work and therefore explained in details as follows. It is to note that propagation as to state estimation occurs block-wise at the highest resolution level. Decomposition of the states by wavelet transform and reconstruction by inverse wavelet transform is effective in this scheme due to better estimation of the error covariance as to the state estimation as explained below.

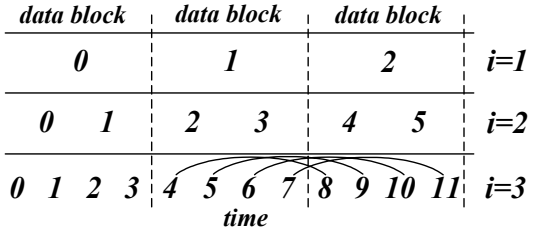

Fig. 2 Measurements at different resolution levels

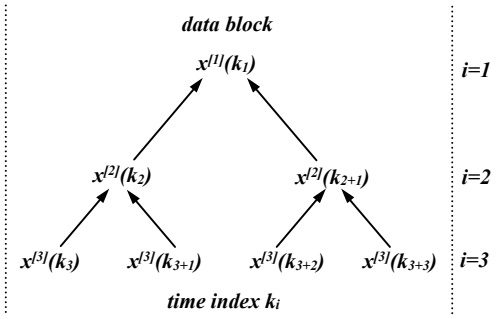

Fig. 3 Wavelet decomposition of state variables in a data block

Within a data block, the state variables at resolution level *i* are designated as

$$X_m^{[i]} = \begin{bmatrix} x^{[i]}k(i) \\ x^{[i]}k(i+1) \\ ..... \\ x^{[i]}k(i+2^{i-1}) \end{bmatrix} \tag{21}$$

$$x^{[i]}k(i) = \begin{bmatrix} x_{k,1}^{[i]} \\ x_{k,2}^{[i]} \\ .... \\ x_{k,s}^{[i]} \end{bmatrix} \tag{22}$$

where *m* is data block index and *s* is the number of state variables. In a data block, there are 2^{i-1} state variables. Each state variable has *s* state components. A lower resolution state variable is computed from

$$x^{[i]}(k_i) = h_1 x^{[i+1]}(k_{i+1}) + h_2 x^{[i+1]}(k_{i+1}+1) \tag{23}$$

where h_1 and h_2 are the Haar low-pass filter coefficients. The details component i.e., high frequency part after the decomposition is computed via

$$y^{[i]}(k_i) = g_1 x^{[i+1]}(k_{i+1}) + g_2 x^{[i+1]}(k_{i+1}+1) \tag{24}$$

where g_1 and g_2 are the Haar high-pass filter coefficients. The reconstruction of the states is carried out by combining (22) and (23) in a matrix equation form as given below.

$$\begin{bmatrix} x^{[i+1]}(k_{i+1}) \\ x^{[i+1]}(k_{i+1}+1) \end{bmatrix} = \boldsymbol{h}^T x^{[i]}(k_i) + \boldsymbol{g}^T y^{[i]}(k_i) \tag{25}$$

Wavelet decomposition and reconstruction is carried out according to the scheme shown in figures 4 and 5.

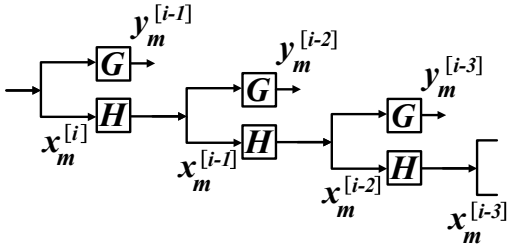

Fig. 4 Wavelet decomposition of state variables in a data block

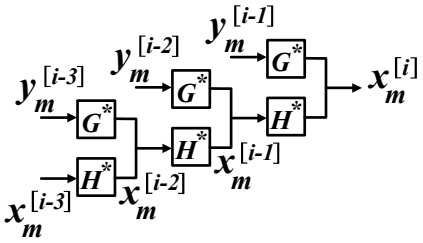

Fig. 5 Wavelet reconstruction of state variables in a data block

The wavelet matrix operator G and the scaling matrix operator H in the decomposition and their counterparts G^* and H^* in the reconstruction contain two-tap Haar filters and they are related by

$$G^* = G^T \qquad H^* = H^T \tag{26}$$

It is to note that the state variable estimations are carried out at the respective resolution levels, as follows.

$$H^{i+1\to i} = diag\{(1/\sqrt{2})h_h^{(1)}, (1/\sqrt{2})h_h^{(2)}, ..., (1/\sqrt{2})h_h^{(K)}\} \tag{27}$$

where K is the number of filters involved in a decomposition from the resolution level i+1 to i. For instance from 2 to 1, then i=1, and K is given by

$$K = 2^{i-1} = 1 \tag{28}$$

as this is seen in figure 2, as the block length is 2. For the *s* state variable of the system, the *H* matrix is composed of *s* Haar filters at the diagonal as

$$H = diag\{H_{[1]}^{\ i+1\to i}, H_{[2]}^{\ i+1\to i}, ..., H_{[K]}^{\ i+1\to i}\} \tag{29}$$

Similarly, for the reconstruction filter, we write

$$G^{i+1\to i} = diag\{(\sqrt{2})g_h^{(1)}, (\sqrt{2})g_h^{(2)}, ..., (\sqrt{2})g_h^{(K)}\} \tag{30}$$

$$G = diag\{G_{[1]}^{\ i+1\to i}, G_{[2]}^{\ i+1\to i}, ..., G_{[K]}^{\ i+1\to i}\} \tag{31}$$

As K is given by (27). For the inverse transform scheme given by figure 5, we write

$$H^* = diag\{H_{[1]}^{\ i\to i+1}, H_{[2]}^{\ i\to i+1}, ..., H_{[K]}^{\ i\to i+1}\} \tag{32}$$

$$G^* = diag\{G_{[1]}^{\ i\to i+1}, G_{[2]}^{\ i\to i+1}, ..., G_{[K]}^{\ i\to i+1}\} \tag{33}$$

where

$$H^{i\to i+1} = diag\{(\sqrt{2})h_h^{T(1)}, (\sqrt{2})h_h^{T(2)}, ..., (\sqrt{2})h_h^{T(K)}\} \tag{34}$$

$$G^{i\to i+1} = diag\{(1/\sqrt{2})g_h^{T(1)}, (1/\sqrt{2})g_h^{T(2)}, ..., (1/\sqrt{2})g_h^{T(K)}\} \tag{35}$$

Above T indicates transpose and K is given by (28).

2.3.1. Example block-wise 2-way multiresolutional computation

An example block wise wavelet computation is presented in this subsection. For this we consider figure 2 and the initial data block designated as 0 with the data samples as x_0 and x_1 at the resolution level i=2. Also for the sake of simplicity we consider s=2; namely only two state variables of the system. Therefore the data samples are denoted as x_{01}, x_{02} and x_{11}, x_{12}; first index is for the data sample, second index for the state variable. We define an auxiliary matrix L as follows

$$L^{[2]} = \begin{bmatrix} 1 & 0 & 0 & 0 \\ 0 & 0 & 1 & 0 \\ 0 & 1 & 0 & 0 \\ 0 & 0 & 0 & 1 \end{bmatrix} \tag{36}$$

which yields

$$L^{[2]}X_m^{[2]} = \begin{bmatrix} 1 & 0 & 0 & 0 \\ 0 & 0 & 1 & 0 \\ 0 & 1 & 0 & 0 \\ 0 & 0 & 0 & 1 \end{bmatrix} \begin{bmatrix} x_{01}^{[2]} \\ x_{02}^{[2]} \\ x_{11}^{[2]} \\ x_{12}^{[2]} \end{bmatrix} = \begin{bmatrix} x_{01}^{[2]} \\ x_{11}^{[2]} \\ x_{02}^{[2]} \\ x_{12}^{[2]} \end{bmatrix} \tag{37}$$

where m is index of the data block which is m=0, above. It is to note that, the sate variables are grouped slightly different for computational convenience; namely the decomposition is carried out by

$$X_m^{[i-1]} = L^{T\,[i-1]} H\, L^{[i]} X_m^{[i]} \tag{38}$$

$$Y_m^{[i-1]} = L^{T\,[i-1]} G\, L^{[i]} X_m^{[i]} \tag{39}$$

where Y_m are the wavelet coefficients. From the definition given by (27) and (30)

$$H^{i+1\to i} = diag\{(1/\sqrt{2})h_h^{(1)}\} = \begin{bmatrix} 1/2 & 1/2 \end{bmatrix} \tag{40}$$

$$G^{i+1\to i} = diag\{(\sqrt{2})g_h^{(1)}\} = \begin{bmatrix} 1 & -1 \end{bmatrix} \tag{41}$$

Also from (29) and (31)

$$G = diag\{G_{[0]}^{\ i+1\to i}, G_{[1]}^{\ i+1\to i}\}$$
$$H = diag\{H_{[0]}^{\ i+1\to i}, H_{[1]}^{\ i+1\to i}\} \tag{42}$$

In (34) substituting i=2, the decomposition at the level i=1, becomes

$$X_0^{[1]} = L^{T\,[1]} H\, L^{[2]} X_m^{[2]} = \begin{bmatrix} 1 & 0 \\ 0 & 1 \end{bmatrix} \begin{bmatrix} .5 & .5 & 0 & 0 \\ 0 & 0 & .5 & .5 \end{bmatrix} \times \begin{bmatrix} 1 & 0 & 0 & 0 \\ 0 & 0 & 1 & 0 \\ 0 & 1 & 0 & 0 \\ 0 & 0 & 0 & 1 \end{bmatrix} \times \begin{bmatrix} x_{01}^{\ [2]} \\ x_{02}^{\ [2]} \\ x_{11}^{\ [2]} \\ x_{12}^{\ [2]} \end{bmatrix} = \begin{bmatrix} .5x_{01}^{[2]} + .5x_{11}^{[2]} \\ .5x_{02}^{[2]} + .5x_{12}^{[2]} \end{bmatrix} \tag{43}$$

which is a low-pass filtered data block by averaging. The wavelet coefficients which are the high-pass filtered data samples are obtained in a similar way as

$$Y_0^{[1]} = L^{T\,[1]} G\, L^{[2]} X_m^{[2]} = \begin{bmatrix} 1 & 0 \\ 0 & 1 \end{bmatrix} \begin{bmatrix} 1 & -1 & 0 & 0 \\ 0 & 0 & 1 & -1 \end{bmatrix} \times \begin{bmatrix} 1 & 0 & 0 & 0 \\ 0 & 0 & 1 & 0 \\ 0 & 1 & 0 & 0 \\ 0 & 0 & 0 & 1 \end{bmatrix} \times \begin{bmatrix} x_{01}^{\ [2]} \\ x_{02}^{\ [2]} \\ x_{11}^{\ [2]} \\ x_{12}^{\ [2]} \end{bmatrix} = \begin{bmatrix} x_{01}^{[2]} - x_{11}^{[2]} \\ x_{02}^{[2]} - x_{12}^{[2]} \end{bmatrix} \tag{44}$$

(43) and (44) are the multiresolutional decomposition of the data block 0, from level i=2 to the level i=1.

The inverse wavelet transform is carried out according to the general scheme given by figure 5.

$$X_m^{[i]} = L^{T\,[i]} H^*\, L^{[i]} X_m^{[i-1]} + L^{T\,[i]} G^*\, L^{[i-1]} Y_m^{[i-1]} \tag{45}$$

From (32) and (33), we write

$$H^* = diag\,\{H_{[1]}^{\ 1\to 2}, H_{[2]}^{\ 1\to 2}\} = \begin{bmatrix} \begin{bmatrix} 1 \\ 1 \end{bmatrix} \begin{bmatrix} 0 \\ 0 \end{bmatrix} \\ \begin{bmatrix} 0 \\ 0 \end{bmatrix} \begin{bmatrix} 1 \\ 1 \end{bmatrix} \end{bmatrix} \tag{46}$$

$$G^* = diag\{G_{[1]}^{\ 1\to 2}, G_{[2]}^{\ 1\to 2}\} = \begin{bmatrix} \begin{bmatrix} .5 \\ -.5 \end{bmatrix} \begin{bmatrix} 0 \\ 0 \end{bmatrix} \\ \begin{bmatrix} 0 \\ 0 \end{bmatrix} \begin{bmatrix} .5 \\ -.5 \end{bmatrix} \end{bmatrix} \tag{47}$$

so that, (45) becomes

$$X_0^{[2]} = L^{T\,[2]} H^*\, L^{[1]} X_0^{[1]} + L^{T\,[2]} G^*\, L^{[1]} Y_0^{[i]} \tag{48}$$

The substitution of the respective matrices into (48) yields

$$\begin{bmatrix}1&0&0&0\\0&0&1&0\\0&1&0&0\\0&0&0&1\end{bmatrix}\left[\begin{bmatrix}1\\1\end{bmatrix}\begin{bmatrix}0\\0\end{bmatrix}\right]\begin{bmatrix}1&0\\0&1\end{bmatrix}\begin{bmatrix}.5x_{01}^{2}+.5x_{11}^{[2]}\\.5x_{02}^{[2]}+.5x_{12}^{[2]}\end{bmatrix}+$$

$$\begin{bmatrix}1&0&0&0\\0&0&1&0\\0&1&0&0\\0&0&0&1\end{bmatrix}\left[\begin{bmatrix}.5\\-.5\end{bmatrix}\begin{bmatrix}0\\0\end{bmatrix}\right]\begin{bmatrix}1&0\\0&1\end{bmatrix}\begin{bmatrix}x_{01}^{2}-x_{11}^{[2]}\\x_{02}^{[2]}-x_{12}^{[2]}\end{bmatrix}= \tag{49}$$

$$\begin{bmatrix}1&0\\0&1\\1&0\\0&1\end{bmatrix}\begin{bmatrix}.5x_{01}^{[2]}+.5x_{11}^{[2]}\\.5x_{02}^{[2]}+.5x_{12}^{[2]}\end{bmatrix}+\begin{bmatrix}.5&0\\0&.5\\-.5&0\\0&-.5\end{bmatrix}\begin{bmatrix}x_{01}^{[2]}-x_{11}^{[2]}\\x_{02}^{[2]}-x_{12}^{[2]}\end{bmatrix}=\begin{bmatrix}.5x_{01}^{[2]}+.5x_{11}^{[2]}\\.5x_{02}^{[2]}+.5x_{12}^{[2]}\\.5x_{01}^{[2]}+.5x_{11}^{[2]}\\.5x_{01}^{[2]}+.5x_{12}^{[2]}\end{bmatrix}+\begin{bmatrix}.5x_{01}^{[2]}-.5x_{11}^{[2]}\\.5x_{02}^{[2]}-.5x_{12}^{[2]}\\-.5x_{01}^{[2]}+.5x_{11}^{[2]}\\-.5x_{01}^{[2]}+.5x_{12}^{[2]}\end{bmatrix}=\begin{bmatrix}x_{01}^{[2]}\\x_{02}^{[2]}\\x_{11}^{[2]}\\x_{12}^{[2]}\end{bmatrix}$$

which is $X_m[2]$ as given in (37).

For the same decomposition from i=3 to i=2, the auxiliary matrix L is given by

$$L^{[3]}=\begin{bmatrix}1&0&0&0&0&0&0&0\\0&0&1&0&0&0&0&0\\0&1&0&0&0&0&0&0\\0&0&0&1&0&0&0&0\\0&0&0&0&1&0&0&0\\0&0&0&0&0&0&1&0\\0&0&0&0&0&1&0&0\\0&0&0&0&0&0&0&1\end{bmatrix} \tag{50}$$

For this case i=2, and K is given by

$$K=2^{i-1}=2 \tag{51}$$

as this is seen in figure 2, where the block length is 4.

2.3.2 Estimate updating

The basic update scheme for dynamic multiresolutional filtering is shown in Fig. 6 where at each resolutional level, when the measurement is available, the state variables are updated and when the block is complete the inverse wavelet transform and fusion is performed. During the inverse transformation wavelet coefficients $Y_{m+1|m+1}[i]$ saved aside are used.

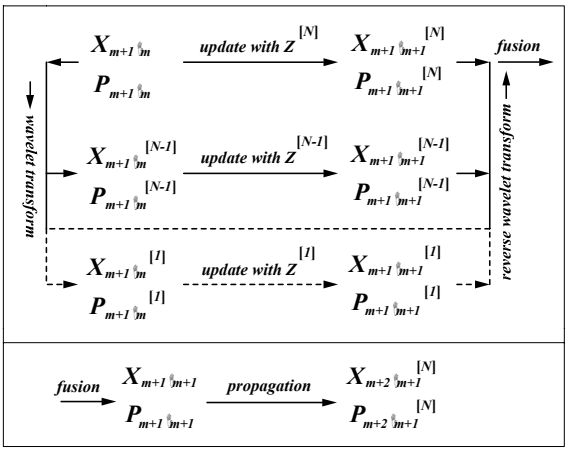

Fig. 6 Wavelet decomposition of state variables in a data block

Explicitly

$$P_{m+1|m}^{[i]} = \begin{bmatrix} P_{XXm+1|m}^{[i]} & P_{XYm+1|m}^{[i]} \\ P_{YXm+1|m}^{[i]} & P_{YYm+1|m}^{[i]} \end{bmatrix} \tag{52}$$

$$X_{m+1|m+1}^{[i]} = X_{m+1|m}^{[i]} + K_{m+1}^{[i]}(Z_{m+1}^{[i]} - C_{m+1}^{[i]} X_{m+1|m}^{[i]}) \tag{53}$$

and

$$P_{XXm+1|m+1}^{[i]} = (I - K_{m+1}^{[i]} C_{m+1}^{[i]}) P_{XXm+1|m}^{[i]} \tag{54}$$

As $X_{m+1|m}^{[i]}$ and $Y_{m+1|m}^{[i]}$, $Y_{m+1|m}^{[i+1]}$ are correlated, the covariance matrices $P_{XYm+1|m}^{[i]}$ and $P_{YXm+1|m}^{[i]}$ are also updated. However, the wavelet coefficients $Y_{m+1|m}^{[i]}$ and their covariance matrices $P_{YYm+1|m}^{[i]}$ are not updated. The minimum variance Kalman gain matrix $K_{m+1}^{[i]}$ at each level, is determined by

$$K_{m+1}^{[i]} = P_{XXm+1|m}^{[i]} C_{m+1}^{[i]T} \left(C_{m+1}^{[i]} P_{XXm+1|m}^{[i]} C_{m+1}^{[i]T} + R_{m+1}^{[i]} \right)^{-1} \tag{55}$$

where the measurent matrix $C_{m=1}^{[i]}$ and $R_{m+1}^{[i]}$ are given by

$$C_{m+1}^{[i]} = diag \begin{bmatrix} C^{[i]}[(m+1)2^{i-1}], C^{[i]}[(m+1)2^{i-1} - 2^{i-1} + 1], \ldots, \\ \ldots\ldots \qquad\qquad , C^{[i]}[(m+1) + 2^{i-1} + 1] \end{bmatrix} \tag{56}$$

$$R_{m+1}^{[i]} = diag\begin{bmatrix} R^{[i]}[(m+1)2^{i-1}], R^{[i]}[(m+1)2^{i-1} - 2^{i-1} + 1], \ldots, \\ \ldots\ldots \qquad\qquad , R^{[i]}[(m+1) + 2^{i-1} + 1] \end{bmatrix} \tag{57}$$

Once, within the moving window, the sequences of updated state variables and error covariances $X_{m+1|m+1}^{[N,i]}$ and $P_{m+1|m+1}^{[N,i]}$ for *i=1,2,..,N* are determined, they must be fused to generate an optimal $X_{m+1|m+1}^{[NF]}$ and $X_{m+1|m+1}^{[NF]}$. $X_{m+1|m+1}^{[NF]}$ and $X_{m+1|m+1}^{[NF]}$. For the minimum fusion error covariance $X_{m+1|m+1}^{[NF]}$, the fused estimate $X_{m+1|m+1}^{[NF]}$ is calculated as

$$X_{m+1|m+1}^{[NF]} = P_{m+1|m+1}^{[NF]}\left[\sum_{i=1}^{N}\left(P_{m+1|m+1}^{[N,i]}\right)X_{m+1|m}^{[N,i]} - \right] \ (N-1)\left(P_{m+1|m}^{[N]}\right)^{-1} X_{m+1|m}^{[N]} \tag{58}$$

where the minimum fusion error covariance $P_{m+1|m+1}^{[NF]}$ becomes

$$\left(P_{m+1|m+1}^{[NF]}\right)^{-1} = \sum_{i=1}^{N}\left(P_{m+1|m+1}^{[N,i]}\right)^{-1} - (N-1)\left(P_{m+1|m}^{[N]}\right)^{-1}. \tag{59}$$

The fused estimate $X_{m+1|m+1}^{[NF]}$ is a weighted summation of both predicted $X_{m+1|m}^{[N]}$ and updated $X_{m+1|m+1}^{[N,i]}$, for i=1,2,..,N. The sum of the weight factors equal to the identity I. This can be seen by substitution of $P_{m+1|m+1}^{[NF]}$ given above into the expression of $X_{m+1|m+1}^{[NF]}$ in (58).

3. Autonomous Robot Navigation

The computer experiments have been carried out with the simulated robot navigation. The state variables vector is given by (22) while taking i=N.

$$x^{[N]}k(N) = \begin{bmatrix} x_{k,1}^{[N]} \\ x_{k,2}^{[N]} \\ \ldots. \\ x_{k,s}^{[N]} \end{bmatrix} \tag{60}$$

Explicitly,

$x^{[N]}k(N) = [x, \dot{x}, y, \dot{y}, \omega]$

where ω is the angular rate and it is estimated during the move. When the robot moves in a straight line, the angular rate becomes zero. The other state variables are x and y coordinates and the respective velocities.

The experiments are carried out as follows. For a pre-defined trajectory, perception measurements along the trajectory are obtained in a virtual reality environment. This trajectory is designated as reference. The measurements as data samples are used in sequence for a real-time robot navigation by multiresolutional dynamic filter estimation. Designing the experiment in this way allows one to assess the effectiveness of the robot navigation by comparison of the actual navigation path with the estimated one. The overall robot trajectory is shown in figure 7 where there are three lines plotted but only two of them are visible. The line marked by * sign represents the measurement data set. The line marked by • is the multiresolutional dynamic filter estimation. The line indicated by o sign is the reference trajectory. These lines are not explicitly seen in the figure. For explicit illustration of the experimental outcomes the same figure with a different zooming ranges and the zooming powers are given in figures 8-12.

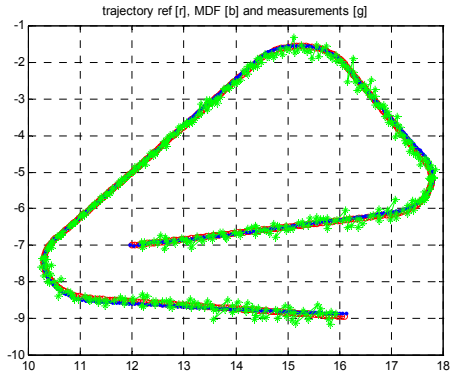

Fig. 7 The overall Robot trajectory with measurement (* signs), and multiresolutinal dynamic filter estimation (• signs).

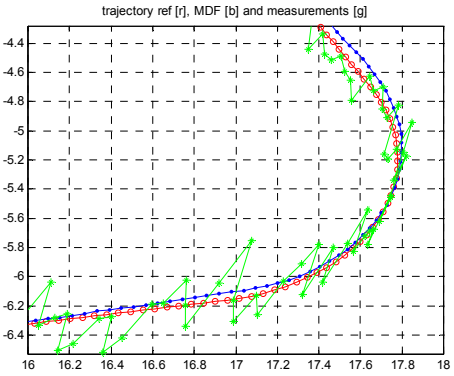

Fig. 8 Enlarged robot trajectory, measurement, and multiresolutinal dynamic filter estimation in angular velocity mode. The * sign is for measurement, o sign for the reference and • sign is the estimated trajectory.

From the experiments it is seen that, the multiresolutional filtering is effective for estimation of the trajectory from perception measurement. Estimations are more accurate in the straight-ahead mode seen in figure 12, compared to the cases where angular velocity does not vanish. This can be explained by noting that in the straight-ahead mode the angular velocity is zero and the system matrix is fixed. However in the non-linear mode the system matrix is approximate due to the estimation error of the angular velocity. In this case the slight difference between the reference trajectory and the estimated trajectory is markedly seen due to the approximation error caused by the Taylor's series expansion and ensuing linearization in (extended) Kalman filtering.

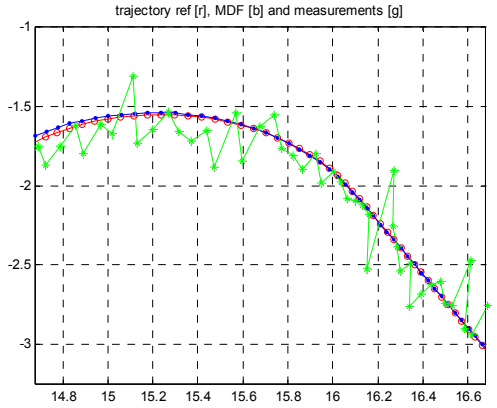

Fig. 9 Enlarged Robot trajectory, measurement multiresolutinal dynamic filter in angular velocity mode. The * sign is for measurement, o sign for the reference and • sign is the estimated trajectory.

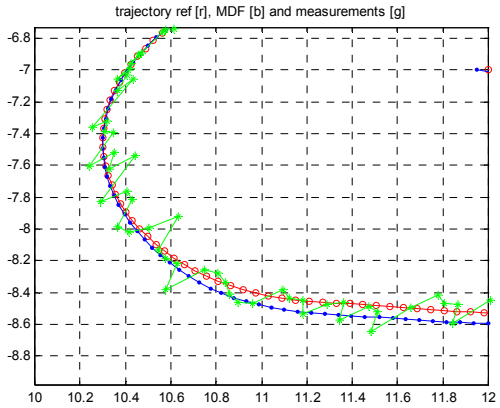

Fig. 10 Enlarged Robot trajectory, measurement multiresolutinal dynamic filter in angular velocity mode. The * sign is for measurement, o sign for the reference and • sign is the estimated trajectory.

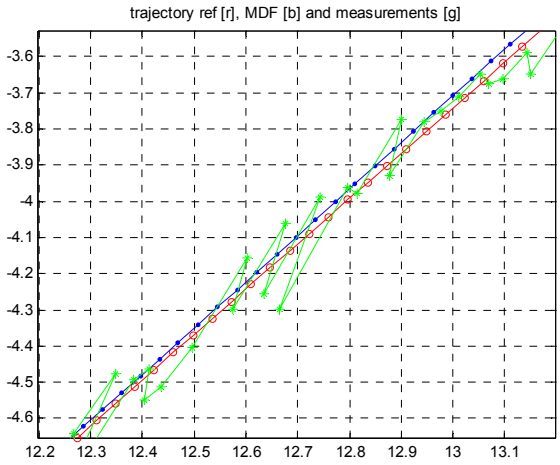

Fig. 11 Enlarged robot trajectory, measurement multiresolutinal dynamic filter straight-ahead mode. The * sign is for measurement, o sign for the reference and • sign is the estimated trajectory.

4. Discussion and Conclusion

The detailed description of processing of spatial information for a perceptual robot is described. Especially, the perception is considered to be a probabilistic concept and defined as such (Ciftcioglu, Ö., Bittermann, M.S. et al., 2006) so that the probabilistic consideration in perceptual robot is desirable for human-like robot navigation. This facilitates the robotic movement coupling the cognition of a robot with the environment. In this context, Bayesian perception and cognition studies (Knill, D.C. & Richards, W., 1996) can be more substantiated with more accurate priors. This is especially important when one deals with a certain scene but from a different vantage point.

In vision robotics autonomous navigation is a challenging issue. Using the perceptual spatial information vision robot can navigate autonomously by perception-based sensory information so that it can react better with respect to the environmental and circumstantial situations. Better is in the sense of obstacle avoidance and way finding without crash. In the present work, the processing the spatial information is accomplished by means of wavelet technology that is the main component in the information fusion process. The simplest form of wavelets is used to cope with the real-time requirements in the navigation and it is demonstrated that, this choice is justified. Kalman filtering is the machinery for the fusion process, as well as it plays the role of optimal observer (Friedland, B., 1986) of the measurements referring to distance (r), angle (θ) and the scalar velocity (v). These may partly be computed from the estimated state variables, in the case of unavailable actual measurement counterparts. For that matter, it is the angular velocity for which the measurements are unavailable, in this work. The work is a clear demonstration of the working state observers and therefore an important hint for the physical robotics exercises.

It is reminded that, the present work is an autonomous robotics simulation implemented in a virtual reality and the results reported are the computer experiments.

Applications of vision robot are countless and they are well documented in the literature. Autonomous robotics with perception is a new dimension in a vision robot as such its vision can be shaped for application dependent vision properties. The investigations presented in this work are motivated by measuring the perception aspects of an architectural design from different vantage points and altogether to obtain a compromise among them, as to a final decision-making for that design. Such a task in one hand is a routine work for a robot in virtual reality and the actual (real) scene having been represented in the virtual reality, the scene can be perceived in many different ways as desired. The same task for a human is in the first place extremely tedious but more importantly subjective in terms of perception measurement and therefore can be deemed to be inconclusive due to probable inconsistencies among different observers and even for a single viewer. This is because of the complexity of the task due to the number of objects involved in the scene. Here the objects may be a number of dwelling units subject to marketing by a building project developer. Since a number of locations and architectural requirements impose condition on perception aspects, the task is a multi-objective optimization subject to these impositions as constraints. Also, in this situation one is interested in a solution on a Pareto front. Such complexities are today effectively dealt with thanks to evolutionary algorithms (Deb, K., 2001; Coello, C.A.C., Veldhuizen, D.A. et al., 2003; Sato, H., Aguirre, H.E. et al., 2007). Some endeavours in the context of architecture are reported in (Bittermann, M., Sariyildiz, I.S. et al., 2008; Ciftcioglu, O. & Bittermann, M.S., 2008). The present research is another endeavour along this line revealing the exhaustive details of spatial information fusion as to accurate robot navigation using multiresolutional dynamic filter approach.

8. References

Anderson, B. D. O. & J. B. Moore (1979). Optimal Filtering. Prenctice-Hall, 0-13-638122-7, Englewood Cliffs, New Jersey

Beetz, M., T. Arbuckle, et al. (2001). Integrated, plan-based control of autonomous robots in human environments. IEEE Intelligent Systems Vol. 16, No. 5, 56-65,

Bittermann, M., I. S. Sariyildiz, et al. (2008). Performance-Based Pareto Optimal Design. Proceedings of Tools and Methods of Competitive Engineering (TMCE), Izmir

Brown, R. G. & Y. C. Hwang (1997). Introduction to Random Signals and Applied Kalman Filtering: With MATLAB Exercises and Solutions, 3rd ed. Wiley, 0-471-12839-2, New York

Ciftcioglu, O. & M. S. Bittermann (2008). Solution Diversity in Multi-Objective Optimization: A study in Virtual Reality. Proceedings of IEEE World Congress on Computational Intelligence, Hong Kong, IEEE

Ciftcioglu, Ö., M. S. Bittermann, et al. (2006). Towards computer-based perception by modeling visual perception: a probabilistic theory. Proceedings of 2006 IEEE Int. Conf. on Systems, Man, and Cybernetics, pp. 5152-5159, Taipei, Taiwan

Ciftcioglu, Ö., M. S. Bittermann, et al. (2007). Visual perception theory underlying perceptual navigation.In: Emerging Technologies, Robotics and Control Systems S. Pennacchio, 139-153 Palermo, International Society for Advanced Research. 1, Palermo

Coello, C. A. C., D. A. Veldhuizen, et al. (2003). Evolutionary Algorithms for Solving Multiobjective Problems. Kluwer Academic Publishers, Boston

Deb, K. (2001). Multiobjective Optimization using Evolutionary Algorithms. John Wiley & Sons,

Friedland, B. (1986). Control System Design. McGraw-Hill, London

Hong, L. (1993). Multiresolutional filtering using wavelet transform. IEEE Trans. on Aerospace and Electronic Systems Vol. 29, No. 4, 1244-1251,

Hong, L. (1994). Multiresolutional multiple model target tracking. IEEE Tranasctions on Aerospace and Electronic Systems Vol. 30, No. 2, 518-524,

Hsin, H. C. & A. C. Li (2006). Wavelet-Based Kalman Filtering in Scale Space for Image Fusion.In: Pattern Recognition and Computer Vision. C. H. Chen and P. S. P. WangSingapore, World Scientific, Singapore

Knill, D. C. & W. Richards (1996). Perception as Bayesian Inference. Cambridege University Press, Cambridge

Mallat, S. (1999). A Wavelet Tour of Signal Processing. Associated Press, New York

Mallat, S. G. (1989). A theory for multiresolution signal decomposition:the wavelet representation. IEEE Trans. on Pattern Analysis and Machine Intelligence Vol. 11, No. 7, 674-693,

Maybeck, P. S. (1979). Stochastic Models, Estimation and Control, Vol I. Academic Press, New York

Ogden, T. (1997). Essential Wavelets for Statistical Applications and Data Analysis. Birkhauser, Boston

Oriolio, G., G. Ulivi, et al. (1998). Real-time map building and navigation for autonomous robots in unknown environments. IEEE Trans. on Systems, Man and Cybernetics - Part B: Cybernetics Vol. 28, No. 3, 316-333,

Percival, D. B. & A. T. Walden (2000). Wavelet Methods for Time Series Analysis. Cambridge University Press,

Sato, H., H. E. Aguirre, et al. (2007). Controlling dominance area of solutions and its impact on the performance of MOEAs.In: Lecture Notes on Computer Science, Evolutionary Multi-Criterion OptimizationHeidelberg, Springer, Heidelberg

Shalom, Y. B., X. R. Li, et al. (2006). Estimation and Application to Tracking and Navigation. Wiley, 0-471-41655-X, Montreal

Simon, D. (2006). Optimal State Estimation. Wiley Interscience, 13 978-0-471-70858-2, New Jersey

Vidakovic, B. (1999). Statistical Modeling by Wavelets. John Wiley & Sons, Inc, 0-471-29365-2, New York

Wang, M. & J. N. K. Liu (2004). Online path searching for autonomous robot navigation. Proceedings of IEEE Conf. on Robotics, Automation and Mechatronics, pp. 746-751, Singapore

Zarchan, P. & H. Musoff (2005). Fundamentals of Kalman Filtering: A Practical Approach. Amarican Institute of Aeronautics and Astranautics, Inc. (AIAAA), 1-56347-694-0, Virginia 20191-4344